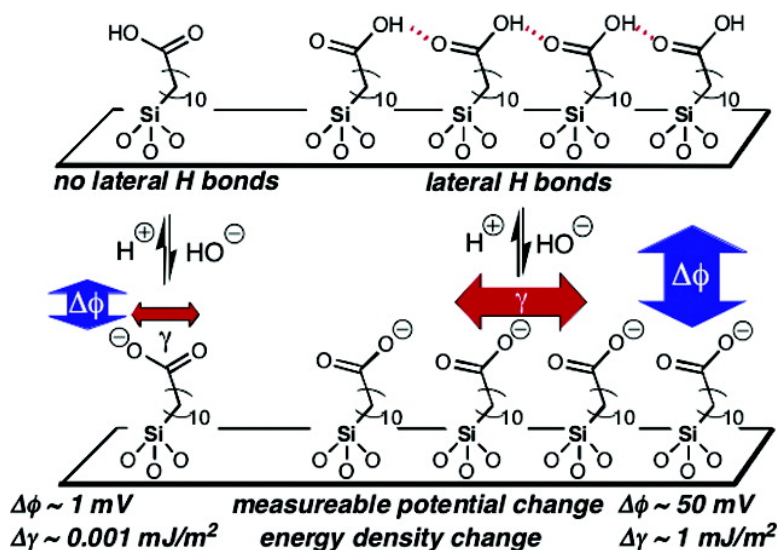


Interfacial Acidities, Charge Densities, Potentials, and Energies of Carboxylic Acid-Functionalized Silica/Water Interfaces Determined by Second Harmonic Generation

Christopher T. Konek, Michael J. Musorrafiti, Hind A. Al-Abadleh,
 Paul A. Bertin, SonBinh T. Nguyen, and Franz M. Geiger

J. Am. Chem. Soc., **2004**, 126 (38), 11754-11755 • DOI: 10.1021/ja0474300 • Publication Date (Web): 28 August 2004

Downloaded from <http://pubs.acs.org> on April 1, 2009



More About This Article

Additional resources and features associated with this article are available within the HTML version:

- Supporting Information
- Links to the 15 articles that cite this article, as of the time of this article download
- Access to high resolution figures
- Links to articles and content related to this article
- Copyright permission to reproduce figures and/or text from this article

[View the Full Text HTML](#)

Interfacial Acidities, Charge Densities, Potentials, and Energies of Carboxylic Acid-Functionalized Silica/Water Interfaces Determined by Second Harmonic Generation

Christopher T. Konek, Michael J. Musorrafiti, Hind A. Al-Abadleh, Paul A. Bertin, SonBinh T. Nguyen, and Franz M. Geiger*

Department of Chemistry, Northwestern University, 2145 Sheridan Road, Evanston, Illinois 60208

Received May 2, 2004; E-mail: geigerf@chem.northwestern.edu

Carboxylic acid-functionalized surfaces have received much attention in the past, as they can control the binding of many solutes important in chemistry, catalysis, environmental science, and biology.^{1–8} Depending on solution pH, acid functional groups can be charged or neutral and thus control the charge state and consequently the potential and the energy density of the aqueous/solid interface, with direct implications for chemical binding and reactivity. Hence, it is critical to quantitatively understand interfacial acidities, potentials, and energies for such functionalized surfaces and interfaces. Second harmonic generation (SHG) is well-suited for this task and has been used in the past to determine surface potentials of metal surfaces,^{9,10} mineral oxide/water interfaces,^{11–13} and charged molecular species at aqueous surfaces.^{14,15}

In this work, we present the first second-harmonic studies that yield the thermodynamic state information for silica/water interfaces decorated with carboxylic acid-functionalized organic adlayers. Using the “ $\chi^{(3)}$ ” method” developed by Eisenthal and co-workers,^{16,17} we determined the changes in interfacial potential ($\Delta\phi$) and surface charge densities ($\Delta\sigma$) for an acid-functionalized silica/water interface. Two acid–base equilibria, whose pK_a values agree with the ones recently reported by Gershevit and Sukenik using ATR-FTIR,¹⁸ are observed. The higher pK_a value is due to the deprotonation of laterally hydrogen-bonded –COOH groups, while the lower one is due to the deprotonation of –COOH groups that are not hydrogen-bonded to one another.¹⁸ By measuring the surface charge density for the acid-functionalized surface, we were able to track the change in interfacial energy density, $\Delta\gamma$, with pH (see Scheme 1). These results provide molecular-level information necessary for understanding and predicting how aqueous-phase species can interact with liquid/solid interfaces decorated with functionalized organic adlayers at a given pH.

Scheme 1. Changes in Interfacial Potential ($\Delta\phi$) and Interfacial Energy Density ($\Delta\gamma$) for Plausible Acid–Base Equilibria Present on Carboxylic Acid-Functionalized Surfaces (Arrow Size Indicates Magnitude)

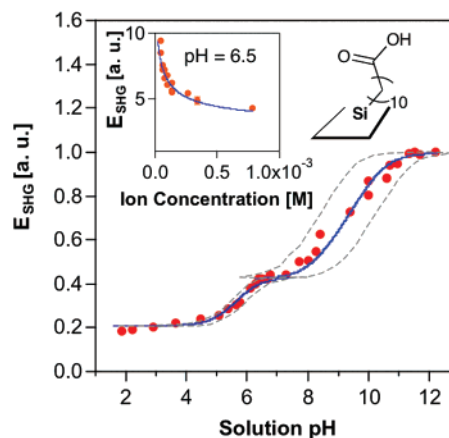
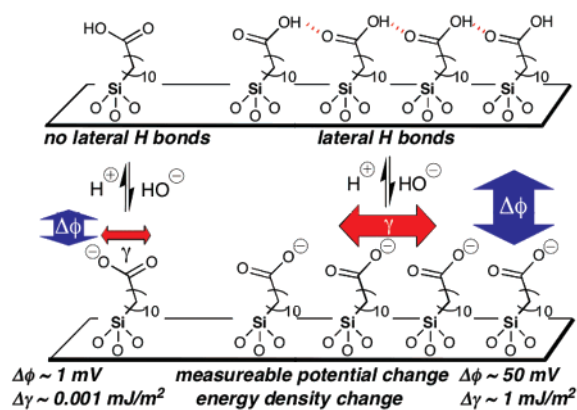


Figure 1. E_{SHG} vs pH at $\lambda_{\text{SHG}} = 290$ nm for an acid-functionalized silica/water interface at room temperature. The dashed lines correspond to 1 standard deviation of the best fit to the pK_a values. The solid line is the pK_a fit. The interfacial potential-dependent second-harmonic electric field, E_{SHG} , is given by $\chi^3 E^2 \phi$, where χ^3 is the third-order susceptibility of the interface, E is the applied electric field, and ϕ is the static interfacial potential. (Inset) E_{SHG} vs bulk salt concentration at $\lambda_{\text{SHG}} = 290$ nm for the acid-functionalized silica/water interface at pH 6.5. These salt concentrations resulted in the data variation necessary for obtaining reasonable fits of the Gouy–Chapman model²³ (solid line).

To minimize the variation in total ion concentration over the pH range studied, our experiments were carried out at a 0.5 mol/L salt concentration. Ester-terminated siloxanes were prepared from the corresponding trichlorosilanes, and hydrolysis of the surface ester groups yielded the acid-functionalized surface.¹⁹ Our recent SHG and SFG measurements are consistent with a high degree of surface functionalization by the siloxanes.¹⁹ Similar to our previous SHG work on chromate binding to silica/water interfaces,^{20,21} the present study was carried out at $\lambda_{\text{probe}} = 580$ nm.

Figure 1 shows the pH dependence of the second-harmonic electric field, E_{SHG} , at 290 nm measured at silica/water interfaces decorated with an acid-functionalized siloxane. The data represent averages of multiple measurements carried out, in no particular pH order, on three different freshly prepared samples, limiting data collection times at high pH to a few minutes.²² There are two inflection points, which are consistent with the existence of two acid–base equilibria at the acid-functionalized silica/water interface.¹⁸

To obtain the surface pK_a values, we determined the maximal surface charge density for each acid–base equilibrium by measuring the second-harmonic field decay with increasing salt concentration at pH 6.5 (inset of Figure 1) and 11.2. By applying the Gouy–Chapman model²³ to fit the data, one obtains maximal surface charge densities, σ_M , of $2.8(5) \times 10^{-4}$ and $4.2(1) \times 10^{-2}$ C/m² at pH 6.5 and 11.2, respectively.²⁴ It is important to note that, even

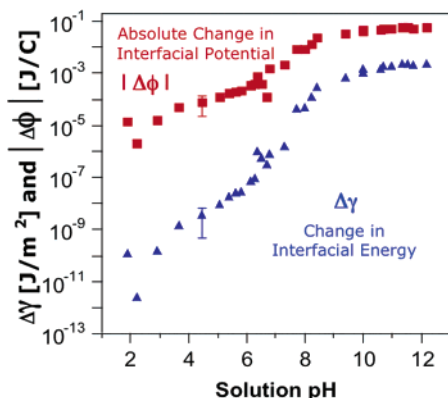


Figure 2. Absolute change in interfacial potential ($|\Delta\phi|$, squares) and change in interfacial energy ($\Delta\gamma$, triangles) of the acid-functionalized silica/water interface as a function of bulk pH. The data at low pH represent the inevitable degradation of signal-to-noise at such low signal intensity levels.

with a high degree of surface functionalization,¹⁹ residual unfunctionalized SiOH groups can still contribute to the surface charge density. Referenced to a surface with 10^{14} singly charged sites per square centimeter, which has a maximal surface charge density of 0.16 C/m^2 , the acid-functionalized surface would have 25% of its surface groups in the deprotonated state at pH 11.2. However, since each acid-terminated siloxane takes up three surface silanol groups on average, the acid-functionalized surface would have 75% of its surface groups in the deprotonated state at pH 11.2.

Applying Eiselenthal's procedure,^{16,17} the data in Figure 1 can be used to determine the $\text{p}K_a$ values for the two acid–base equilibria present at the interface. The first acid–base equilibrium corresponds to a $\text{p}K_a$ value of 5.6 ± 0.2 , and the second one corresponds to a $\text{p}K_a$ value of 9 ± 1 . Our values are within 10% of those reported by Gershevit and Sukenik, who examined the structural aspects of carboxylic acid-terminated self-assembled siloxane monolayers on silicon wafers.¹⁸

For each acid–base equilibrium, the change in interfacial energy density with changing interfacial potential is given by $\Delta\gamma = -\sigma_M f \Delta\phi$,²⁵ where σ_M is again the maximum surface charge density, f is the fraction of ionized surface species at each pH referenced to the lowest charged state, and $\Delta\phi$ is the change in interfacial potential from the lowest charged state. Figure 2 shows the absolute value of the interfacial potential change, $|\Delta\phi|$, and the resulting interfacial energy density change, $\Delta\gamma$. Both values are referenced to the data obtained at the lowest pH examined, which correspond to the highest protonation state at the interface. The effect of solution pH on these two surface parameters is striking: between pH 2 and 12, the interfacial potential changes by 3 orders of magnitude from 10^{-2} mV to several tens of millivolts, and the interfacial energy changes by 7 orders of magnitude. This dramatic increase in interfacial energy with pH is consistent with an increase in electrostatic repulsion among adjacent $-\text{COO}^-$ groups,⁶ which is also reflected by the increase in interfacial charge density as the solution pH increases from 2 to 12. In contrast, the isolated $-\text{COO}^-$ groups result in a much smaller $\Delta\gamma$ and $\Delta\phi$.

The results shown in Figure 2 are in qualitative agreement with AFM-based surface potential measurements reported by Hu and Bard on carboxylic acid-terminated thiols on gold.⁶ On the basis of our data, it is possible to suggest pathways that can control the interaction of aqueous-phase species with polar carboxylic acid-

functionalized liquid/solid interfaces at a given pH. These considerations apply to ionic and polar neutral surfaces. Above pH 5.6, Coulomb interactions between charged surface groups and charged solutes as well as ion–dipole interactions of molecular solutes with ionized surface groups will be important. Below pH 9, ion–dipole interactions between ionic solutes and molecular surface groups as well as chelating and hydrogen-bond interactions involving surface OH groups will be important. Hydrogen bonding involving OH groups in the solute or the solvent can occur in the full pH range covered in this study. An additional driving force for binding to the interface is the lowering of the interfacial energy, which increases with increasing pH.

Our study provided a method for obtaining quantitative interface-specific thermodynamic information, which can be used to rationalize and predict how aqueous-phase species can interact with functionalized organic adlayers on solid surfaces over a wide pH range. This methodology lays the foundation for quantifying the detailed chemical binding parameters of a wide variety of environmental pollutants or biological agents at the molecular level and with high sensitivity.

Acknowledgment. We acknowledge an NSF CAREER Award, the ACS-PRF, the Northwestern University Institute for Environmental Catalysis, and the Northwestern University Nanoscale Science and Engineering Center.

References

- (1) Lahann, J.; Mitragotri, S.; Tran, T.-N.; Kaido, H.; Sundaram, J.; Choi, I. S.; Hoffer, S.; Somorjai, G.; Langer, R. *Science* **2003**, *299*, 371–374.
- (2) Chance, J. J.; Purdy, W. C. *Langmuir* **1997**, *13*, 4487–4489.
- (3) Ikeura, Y.; Kurihara, K.; Kunitake, T. *J. Am. Chem. Soc.* **1991**, *113*, 7342–7350.
- (4) Han, M. Y.; Kane, R.; Goto, M.; Belfort, G. *Macromolecules* **2003**, *36*, 4472–4477.
- (5) Prime, K. J.; Whitesides, G. M. *Science* **1991**, *252*, 1164.
- (6) Hu, K.; Bard, A. J. *Langmuir* **1997**, *13*, 5114–5119.
- (7) Zhou, D. J.; Wang, X. Z.; Birch, L.; Rayment, T.; Abell, C. *Langmuir* **2003**, *19*, 10557–10562.
- (8) Burke, S. E.; Barrett, C. J. *Langmuir* **2003**, *19*, 3297–3303.
- (9) Bradley, R. A.; Georgiadis, R.; Kevan, S. D.; Richmond, G. L. *J. Chem. Phys.* **1993**, *99*, 5535–5546.
- (10) Hewitt, T. D.; Gao, R.; Roy, D. *Surf. Sci.* **1993**, *291*, 233–241.
- (11) Lantz, J. M.; Baba, R.; Corn, R. M. *J. Phys. Chem.* **1993**, *97*, 7392–7395.
- (12) Higgins, S. R.; Stack, A. G.; Knauss, K. G.; Eggleston, C.; Jordan, G. In *Water–Rock Interactions, Ore Deposits, and Environmental Geochemistry: A Tribute to David A. Crerar*; Hellmann, R. E., Ed.; Geochemical Society: St. Louis, MO, 2002; Vol. 7.
- (13) Ong, S.; Zhao, X.; Eiselenthal, K. B. *Chem. Phys. Lett.* **1992**, *191*, 327–335.
- (14) Eiselenthal, K. B. *Chem. Rev.* **1996**, *96*, 1343–1360.
- (15) Zhao, X.; Subrahmanyam, S.; Eiselenthal, K. B. *Chem. Phys. Lett.* **1990**, *171*, 558–562.
- (16) Zhao, X.; Ong, S.; Wang, H.; Eiselenthal, K. B. *Chem. Phys. Lett.* **1993**, *214*, 203–207.
- (17) Yan, E. C. Y.; Liu, Y.; Eiselenthal, K. B. *J. Phys. Chem. B* **1998**, *102*, 6331–6336.
- (18) Gershevit, O.; Sukenik, C. N. *J. Am. Chem. Soc.* **2004**, *126*, 482–483.
- (19) Al-Abadleh, H. A.; Voges, A. B.; Bertin, P. A.; Nguyen, S. T.; Geiger, F. M., submitted.
- (20) Mifflin, A. L.; Gerth, K. A.; Geiger, F. M. *J. Phys. Chem. A* **2003**, *107*, 9620–9627.
- (21) Mifflin, A. L.; Gerth, K. A.; Weiss, B. M.; Geiger, F. M. *J. Phys. Chem. A* **2003**, *107*, 6212–6217.
- (22) Control experiments carried out at pH 12 showed constant SHG signal intensities for approximately 60 min.
- (23) Atkins, P. W. *Physical Chemistry*, 6th ed.; Oxford University Press: Oxford, UK, 1998.
- (24) The former number is technically difficult to measure due to its small magnitude. To the best of our knowledge, our experimental setup is the first that is capable of detecting this quantity.
- (25) Adamson, A. W. *Physical Chemistry of Surfaces*, 5th ed.; John Wiley & Sons: New York, 1990.

JA0474300